ECE 604, Lecture 19

Fri, Feb 22, 2019

Contents

Printed on March 24, 2019 at 16 : 44: W.C. Chew and D. Jiao.

1 Rectangular Waveguides, Contd.

1.1 TM Modes (E Modes or $E_z \neq 0$ Modes)

The above exercise for TE modes can be repeated for the TM modes. The scalar wave function for the TM modes is

$$\Psi_{es}(x,y) = A \sin\left(\frac{m\pi}{a}x\right) \sin\left(\frac{n\pi}{b}y\right) \tag{1.1}$$

Here, sine functions are chosen for the standing waves, and the chosen values of β_x and β_y ensure that the homogeneous Dirichlet boundary condition is satisfied on the entire waveguide wall. Neither of the m and n can be zero, lest the field is zero. In this case, both $m > 0$, and $n > 0$ are needed. Thus, the lowest TM mode is the TM_{11} mode. Notice here that

$$\beta_s^2 = \beta_x^2 + \beta_y^2 = \left(\frac{m\pi}{a}\right)^2 + \left(\frac{n\pi}{b}\right)^2 \tag{1.2}$$

Therefore, the corresponding cutoff frequencies and cutoff wavelengths for the TM_{mn} modes are the same as the TE_{mn} modes. These modes are degenerate in this case. For the lowest modes, TE_{11} and TM_{11} modes have the same cutoff frequency. Figure 1 shows the dispersion curves for different modes of a rectangular waveguide. Notice that the group velocities of all the modes are zero at cutoff, and then the group velocities approach that of the waveguide medium as frequency becomes large.

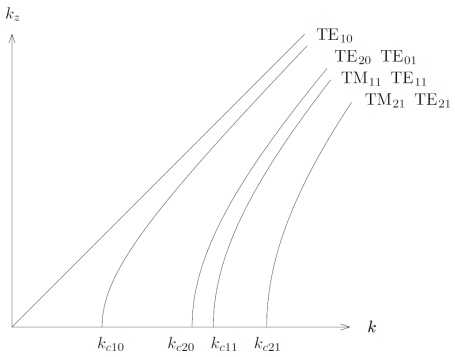

Figure 4.2.18 k_z-k **diagram for guided modes.**

Figure 1: Dispersion curves for rectangular a rectangular waveguide. Notice that the lowest TM mode is the TM_{11} mode, and k is equivalent to β in this course (Courtesy of J.A. Kong).

1.2 Bouncing Wave Picture

We have seen that the transverse variation of a mode in a rectangular waveguide can be expanded in terms of sine and cosine functions which represent standing

waves, or that they are

$$(\exp(-j\beta_x x) \pm \exp(j\beta_x x))\,(\exp(-j\beta_y y) \pm \exp(j\beta_y y))$$

When the above is expanded and together with the $\exp(-j\beta_z z)$ the mode propagating in the z direction, we see four waves bouncing around in the xy directions and propagating in the z direction. The picture of this bouncing wave can be depicted in Figure 2.

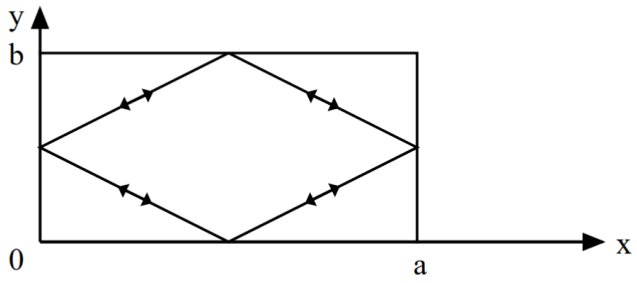

Figure 2:

1.3 Field Plots

Plots of the fields of different rectangular waveguide modes are shown in Figure 3. Higher frequencies are needed to propagate the higher order modes or the high m and n modes. Notice that for higher m's and n's, the transverse wavelengths are getting shorter, implying that β_x and β_y are getting larger because of the higher frequencies involved.

Notice also how the electric field and magnetic field curl around each other. Since $\nabla \times \mathbf{H} = j\omega\varepsilon\mathbf{E}$ and $\nabla \times \mathbf{E} = -j\omega\mu\mathbf{H}$, they do not curl around each other "immediately" but with a $\pi/2$ phase delay due to the $j\omega$ factor. Therefore, the $\mathbf{E}$ and $\mathbf{H}$ fields do not curl around each other at one location, but at a displaced location due to the $\pi/2$ phase difference. This is shown in Figure 4.

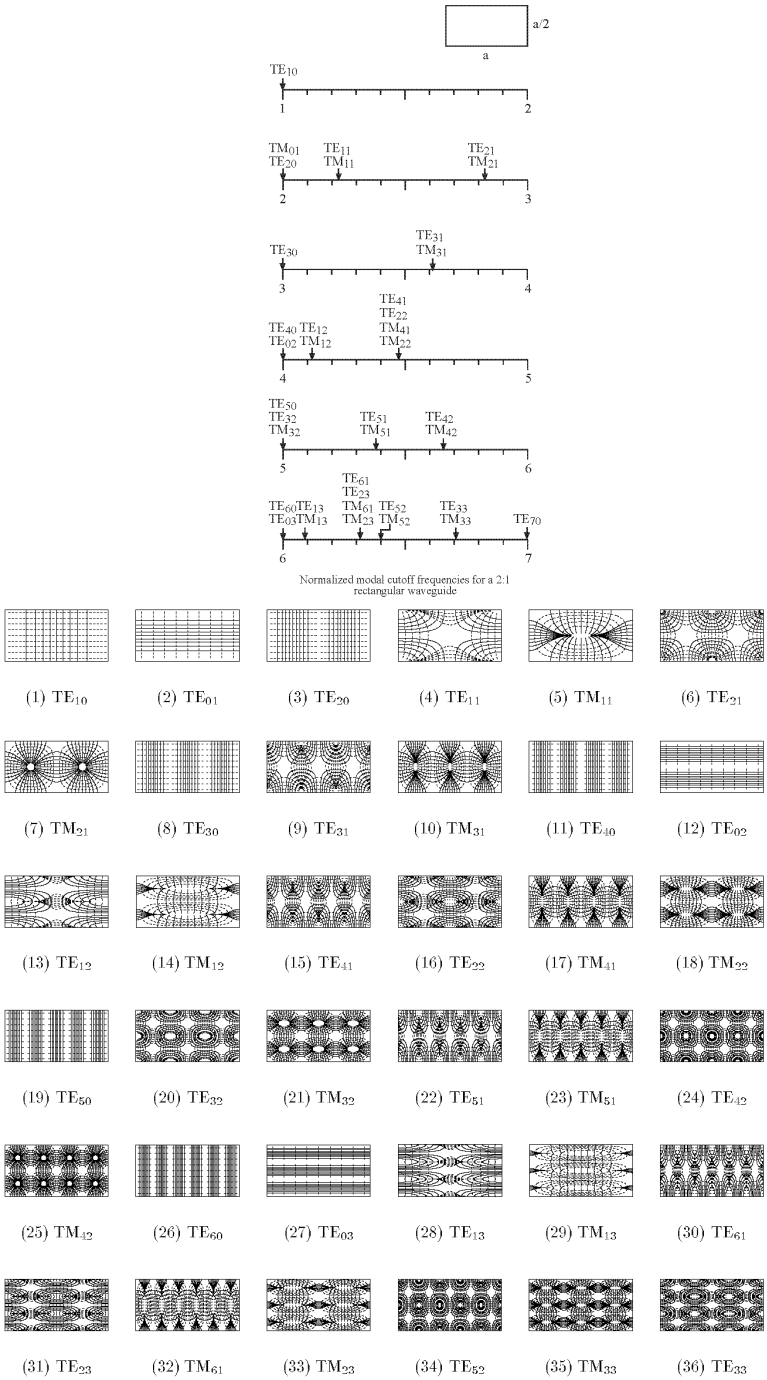

Figure 3: Courtesy of Andy Greenwood. Original plots published in Lee, Lee, and Chuang, IEEE T-MTT, 33.3 (1985): pp. 271-274.

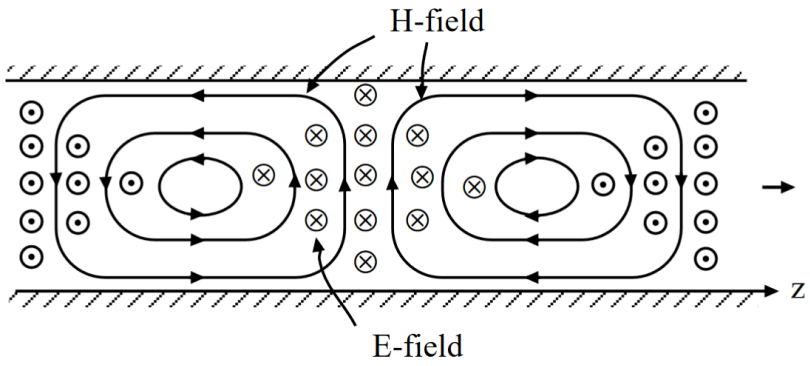

Figure 4:

2 Circular Waveguides

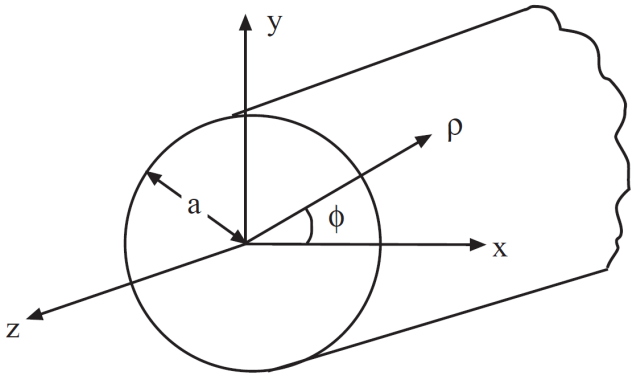

Figure 5:

2.1 TE Case

For a circular waveguide, it is best first to express the Laplacian operator, ${\nabla_s}^2 = \nabla_s \cdot \nabla_s$, in cylindrical coordinates. Doing a table lookup, $\nabla_s \Psi = \hat{\rho}\frac{\partial}{\partial \rho}\Psi + \hat{\phi}\frac{1}{\rho}\frac{\partial}{\partial \phi}$, $\nabla_s \cdot \mathbf{A} = \frac{1}{\rho}\frac{\partial}{\partial \rho}\rho A_\rho + \frac{1}{\rho}\frac{\partial}{\partial \phi}A_\phi$. Then

$$\left({\nabla_s}^2 + {\beta_s}^2\right)\Psi_{hs} = \left(\frac{1}{\rho}\frac{\partial}{\partial \rho}\rho\frac{\partial}{\partial \rho} + \frac{1}{\rho^2}\frac{\partial^2}{\partial \phi^2} + {\beta_s}^2\right)\Psi_{hs}(\rho,\phi) = 0 \qquad (2.1)$$

Using separation of variables, we let

$$\Psi_{hs}(\rho,\phi) = B_n(\beta_s\rho)e^{\pm jn\phi} \tag{2.2}$$

Then $\frac{\partial^2}{\partial\phi^2} \to -n^2$, and (2.1) becomes an ordinary differential equation which is

$$\left(\frac{1}{\rho}\frac{d}{d\rho}\rho\frac{d}{d\rho} - \frac{n^2}{\rho^2} + {\beta_s}^2\right) B_n(\beta_z\rho) \tag{2.3}$$

The above is known as the Bessel equation whose solutions are special functions. These special functions are $J_n(x)$, $N_n(x)$, $H_n^{(1)}(x)$, and $H_n^{(2)}(x)$ which are called Bessel, Neumann, Hankel fuction of the first kind, and Hankel function of the second kind, respectively, where n is the order, and x is the argument.[1] Since this is a second order ordinary differential equation, only two of the four commonly encountered solutions of Bessel equation are independent. Therefore, they can be expressed then in term of each other. Their relationships are shown below:[2]

Bessel, $$J_n(x) = \frac{1}{2}[{H_n}^{(1)}(x) + {H_n}^{(2)}(x)] \tag{2.4}$$

Neumann, $$N_n(x) = \frac{1}{2j}[{H_n}^{(1)}(x) - {H_n}^{(2)}(x)] \tag{2.5}$$

Hankel–First kind, $${H_n}^{(1)}(x) = J_n(x) + jN_n(x) \tag{2.6}$$

Hankel–second kind, $${H_n}^{(2)}(x) = J_n(x) - jN_n(x) \tag{2.7}$$

It can be shown that

$${H_n}^{(1)}(x) \sim \sqrt{\frac{2}{\pi x}}e^{jx - j(n+\frac{1}{2})\frac{\pi}{2}}, \quad x \to \infty \tag{2.8}$$

$${H_n}^{(2)}(x) \sim \sqrt{\frac{2}{\pi x}}e^{-jx + j(n+\frac{1}{2})\frac{\pi}{2}}, \quad x \to \infty \tag{2.9}$$

They correspond to traveling wave solutions when $\rho \to \infty$. Since $J_n(x)$ and $N_n(x)$ are linear superpositions of these traveling wave solutions, they correspond to standing wave solutions. Moreover, $N_n(x)$, ${H_n}^{(1)}(x)$, and ${H_n}^{(2)}(x) \to \infty$ when $x \to 0$. Since the field has to be regular when $\rho \to 0$ at the center of the waveguide shown in Figure 5, the only viable solution for the waveguide is that $B_n(\beta_s\rho) = AJ_n(\beta_s\rho)$. Thus

$$\Psi_{hs}(\rho,\phi) = AJ_n(\beta_s\rho)e^{\pm jn\phi} \tag{2.10}$$

The homogeneous Neumann boundary condition on the waveguide wall then translates to

$$\frac{d}{d\rho}J_n(\beta_s\rho) = 0, \quad \rho = a \tag{2.11}$$

[1] Some textbooks use $Y_n(x)$ for Neumann functions.

[2] Their relations with each other are similar to those between $\exp(-jx)$, $\sin(x)$, and $\cos(x)$.

Defining $J_n{}'(x) = \frac{d}{dx} J_n(x)$, the above is the same as

$$J_n{}'(\beta_s a) = 0 \tag{2.12}$$

Plots of Bessel functions and their derivatives are shown in FIgure **??**. The above are the zeros of the derivative of Bessel function and they are tabulated in many textbooks. The m-th zero of $J_n{}'(x)$ is denoted to be β_{nm} in many books,[3] and some of them are also shown in Figure **??**; and hence, the guidance condition for a waveguide mode is then

$$\beta_s = \beta_{nm}/a \tag{2.13}$$

for the TE_{nm} mode. Using the fact that $\beta_z = \sqrt{\beta^2 - \beta_s^2}$, the corresponding cutoff frequency of the TE_{nm} mode is

$$\omega_{nm,c} = \frac{1}{\sqrt{\mu\varepsilon}} \frac{\beta_{nm}}{a} \tag{2.14}$$

When $\omega < \omega_{nm,c}$, the corresponding mode cannot propagate in the waveguide as β_z becomes pure imaginary. The corresponding cutoff wavelength is

$$\lambda_{nm,c} = \frac{2\pi}{\beta_{nm}} a \tag{2.15}$$

By the same token, when $\lambda > \lambda_{nm,c}$, the corresponding mode cannot be guided by the waveguide.

2.2 TM Case

The corresponding boundary value problem for this case is

$$\left(\frac{1}{\rho} \frac{\partial}{\partial \rho} \rho \frac{\partial}{\partial \rho} + \frac{1}{\rho^2} \frac{\partial^2}{\partial \phi^2} + {\beta_s}^2 \right) \Psi_{es}(\rho, \phi) = 0 \tag{2.16}$$

with the homogeneous Dirichlet boundary condition, $\Psi_{es}(a, \phi) = 0$, on the waveguide wall. The solution is

$$\Psi_{es}(\rho, \phi) = A J_n(\beta_s \rho) e^{\pm jn\phi} \tag{2.17}$$

with the boundary condition that $J_n(\beta_s a) = 0$. The zeros of $J_n(x)$ are labeled as α_{nm} is many textbooks, as well as in Figure **??**; and hence, the guidance condition is that for the TM_{nm} mode is that

$$\beta_s = \frac{\alpha_{nm}}{a} \tag{2.18}$$

With $\beta_z = \sqrt{\beta^2 - \beta_s^2}$, the corresponding cutoff frequency is

$$\omega_{nm,c} = \frac{1}{\sqrt{\mu\varepsilon}} \frac{\alpha_{nm}}{a} \tag{2.19}$$

[3] Notably, Abramowitz and Stegun, Handbook of Mathematical Functions.

or when $\omega < \omega_{nm,c}$, the mode cannot be guided. The cutoff wavelength is

$$\lambda_{nm,c} = \frac{2\pi}{\alpha_{nm}} a \tag{2.20}$$

with the notion that when $\lambda > \lambda_{nm,c}$, the mode cannot be guided.

It turns out that the lowest mode in a circular waveguide is the TE_{11} mode. It is actually a close cousin of the TE_{10} mode of a rectangular waveguide. Table in Figure **??** shows the plot of Bessel function $J_n(x)$ and its derivative $J_n'(x)$.